SCIENCEFORECAST
Connecting Research to Drive Scientific Innovation

Research Article
Published: 17 Sep, 2018

SF Journal of Nanochemistry and Nanotechnology

The Effect of Ag Nanoparticles of Varying Morphology on the Photocatalytic Activity of Ag/Tio$_2$ Nanocomposites

Nyamukamba P[1], Mungondori HH[1], Tichagwa L[2], Petrik L[3] and Okoh O[1]*

[1]Department of Pure and Applied Chemistry, University of Fort Hare, Republic of South Africa

[2]Department of Polymer Technology & Engineering, Harare Institute of Technology, Zimbabwe

[3]Chemistry Department, University of the Western Cape, Bellville, South Africa

Abstract

Attempts to improve the photocatalytic activity of TiO_2 by doping have proven to be challenging due to defect-induced charge trapping and recombination sites of photo-excited charge carriers, which compromise its photocatalytic activity. The use of nanocomposites consisting of TiO_2 and plasmonic nanoparticles seems to be a better alternative. In this study, new nanocomposites consisting of TiO_2 and silver nanomaterials of different shapes and sizes were prepared and the extent to which the silver nanomaterials enhance the photocatalytic activity of TiO_2 was evaluated using methyl orange. All the silver nanomaterials were found to enhance the photocatalytic activity of TiO_2 photocatalyst under UV light. The highest enhancement was achieved by using spherical Ag nanoparticles followed by Ag nanorods and lastly Ag dendrites. The spherical silver nanoparticles exhibited the smallest particle size (5-10 nm) translating to high surface area to volume ratio. The photodegradation intermediates of methyl orange were determined using LC-MS for the first time in the positive mode.

Keywords: Dendrites; Photocatalysis; Nanocomposites; Titanium dioxide; Topography

OPEN ACCESS

Correspondence:
Mungondori Henry Heroe, Department of Pure and Applied Chemistry, University of Fort Hare, 1 King Williams Town Road, Alice 5700, Republic of South Africa.
Tel: *+27605038175*
E-mail: *henrymungondori@gmail.com*

Received Date: *27 Jul 2018*
Accepted Date: *10 Sep 2018*
Published Date: *17 Sep 2018*

Citation: *Nyamukamba P, Mungondori HH, Tichagwa L, Petrik L, Okoh O. The Effect of Ag Nanoparticles of Varying Morphology on the Photocatalytic Activity of Ag/Tio2 Nanocomposites. SF J Nanochem Nanotechnol. 2018; 1(1): 1009.*

ISSN 2643-8135

Copyright *© 2018 Mungondori HH. This is an open access article distributed under the Creative Commons Attribution License, which permits unrestricted use, distribution, and reproduction in any medium, provided the original work is properly cited.*

Introduction

A lot of effort has been devoted to the fabrication of nanostructured materials with tunable properties for applications in advanced catalysis [1]. The intrinsic properties of metal nanoparticles are determined by their shape, size, composition, and crystallinity. Among these properties, the controlling of the shape of metal nanoparticles has been a challenge. The coupling of different nanostructured nanomaterials has been found to improve their technological performances and this has encouraged researchers to explore the possibility of using plasmon metal/titanium dioxide composites in photocatalysis.

In recent years, the photocatalytic degradation of undesirable organic contaminants using TiO_2 photocatalyst to solve environmental problems due to pollution has been widely studied [2,3]. It is a versatile, cost effective, and environmentally friendly technology. The inertness of TiO_2 to chemical environments and its photostability makes it a useful photocatalyst in many practical applications such as environmental clean-up, drinking water treatment and industrial wastewater treatment. Its effectiveness is sometimes limited by much reduced electron-hole separation. Recently, plasmonic nanocomposites have been found to be the centre of attraction for their potential use in photocatalysis so as to reduce electron-hole recombination rates. Among the different plasmonic nanocomposites, those of Ag and TiO_2 have been of interest due to their interesting properties that arise from the localized surface plasmon resonance (SPR) effect [4,5].

The interest in combining silver nanoparticles with TiO_2 photocatalyst relies on silver's ability in acting as a sink for electrons. In particular, when metal nanoparticles are in contact with a TiO_2 semiconductor, there is creation of a Schottky barrier that facilitates movement of electrons from TiO_2 nanoparticles with high Fermi level to silver nanoparticles which have a low Fermi level. This enhances separation of charge carriers and suppresses their recombination rates. The movement of electrons across the Schottky barrier leaves additional positive holes on TiO_2, which are capable of oxidizing organic contaminants.

A lot of effort has been put on improving the photocatalytic activity of TiO_2 by depositing noble metals [6-8]. However, metals such as Pt and Au are expensive to be used on an industrial scale, hence use of Ag is more economical. The effect of silver on titania was investigated and it was

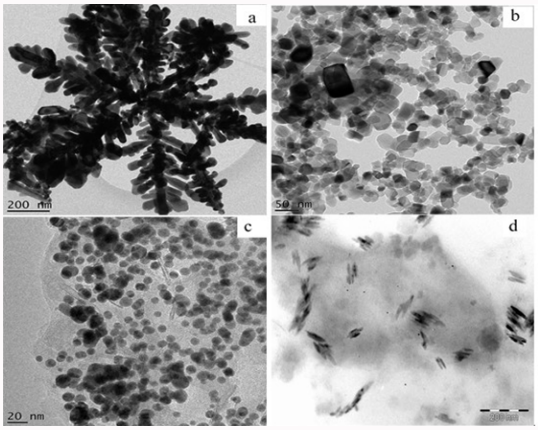

Figure 1: HRTEM images of (a) silver dendritic nanostructures; (b) TiO2 nanoparticles; (c) AgSNPs and (d) TEM image of Ag nanorods.

revealed that the degradation of methylene blue was more efficient with the silver modified TiO_2 compared to pure titania [7].

The aim of this work was to evaluate the effect of different silver nanostructure morphologies and size on TiO_2 photocatalytic activity in the decontamination of water under UV light. Photocatalytic studies on Ag/TiO_2 nanocomposites have been reported in literature [9,10], but according to literature, this is the first attempt to do a comparative study on the effect of silver dendrites, silver nanorods and spherical silver nanoparticles on TiO_2 photocatalytic activity for pollutants removal under UV light irradiation.

Experimental Section

Chemicals and reagents

Silver nitrate (99.8%) from SAARCHEM SA, trisodium citrate ($Na_3C_6H_5O_7$, 99%) supplied by ACE, sodium hydroxide and titanium (IV) tetrachloride (99%) purchased from Merck Germany, polyvinylpyrrolidone (PVP), hydrogen peroxide and sodium borohydride ($NaBH_4$, 96%) were purchased from Sigma Aldrich. All chemicals used in this study were analytical grade and were used as received without further purification. For all the preparations of solutions, deionized water was used.

Materials synthesis

Synthesis of silver dendrites (AgDR): Two drops of hydrogen peroxide were added to 50mL of 0.2mM silver nitrate solution in a conical flask with magnetic stirring. PVP solution (1mL of 8.86mM) was then added drop wise to the solution followed by addition of 6mL of 0.25mM trisodium citrate. The mixture was stirred for thirty minutes before exposure to UV-light of wavelength 366nm for 12 hours. The solution was then aged for 7 days undisturbed at room temperature and the product was then separated from solution by centrifugation.

Synthesis of silver nanorods (AgNR): Silver nitrate (0.04g) was dissolved in 100 mL of deionized water followed by addition of 10mL of 0.03M trisodium citrate with magnetic stirring. PVP solution (5mL of 0.16M) was then added with vigorous stirring followed by 0.2mL of hydrogen peroxide. The pH was adjusted to 9 using sodium hydroxide solution (25% w/v). After 10 minutes of vigorous stirring, 0.5mL of 0.1M sodium borohydride were added drop wise. The reaction medium was then exposed to UV light of wavelength 365nm for 30 minutes. The solution was kept at room temperature under stirring for 24 hours.

Table 1: Sample description and codes of the samples prepared.

Sample description	Sample Code
Pure TiO_2	T1
Spherical silver nanoparticles	AgSNP
Silver dendrites	AgDR
Silver nanorods	AgNR
TiO_2/AgSNP (0.5%wt AgNR) nanocomposite	TAgNR
TiO_2/AgDR (0.5wt% AgDR) nanocomposite	TAgDR
TiO_2/AgNR (0.5%wt AgNR) nanocomposite	TAgNR

Synthesis of spherical silver nanoparticles (AgSNPs): Silver nitrate (0.01g) was dissolved in 33.3mL of deionized water followed by addition of 0.007mmol of trisodium citrate solution and 0.20mmol of PVP solution with vigorous stirring. About 0.2mL of hydrogen peroxide was then added to the reaction solution. After 10 minutes of stirring, 1.7mL of 0.078M sodium borohydride were added drop wise. The solution was then heated at 65°C for 30 minutes and then left to cool to room temperature. Separation of the nanoparticles was achieved by centrifugation.

Synthesis of titanium dioxide (TiO_2) nanoparticles: Titanium dioxide was prepared using a method reported in literature [11]. In a typical experiment 6 mL of titanium tetrachloride was added drop wise to 100mL of distilled water in a flask immersed in an ice bath with vigorous stirring. The pH was adjusted to 8.0 using potassium hydroxide and heated at 95°C for 30 minutes. The precipitate was separated from the solution by centrifugation.

Synthesis of TiO_2/plasmon metal composites: To prepare TiO_2/Ag nanocomposites containing 0.5wt% Ag, 1.99g of TiO_2 were mixed with 10mg of silver nanostructures (AgNR, AgDR and AgSNP) in methanol and sonicated. About 0.02g of the TiO_2/Ag metal nanocomposites were then deposited on quartz supports (2.5cm × 3cm) using a method reported in literature [12]. The sample description and codes of the prepared samples are shown in Table 1.

Evaluation of photocatalytic activity

The photocatalytic activity evaluations of the photocatalysts were performed using methyl orange under UV light irradiation. All photodegradation experiments were conducted at a temperature of 25°C and at pH 7. The photocatalyst coated quartz substrates were immersed in 100mL of 10ppm methyl orange solution. The photocatalysts were placed in such a way that the entire photocatalyst was uniformly irradiated with incident UV light. Aliquots were taken at 30 minute intervals for UV-Vis analysis.

Determination of methyl orange photodegradation products

Liquid chromatography-mass spectrometry was used to determine the photodegradation intermediates and the photodegradation pathway followed by methyl orange. During the photodegradation process at 25°C and pH 7, aliquots were taken from the reaction vessel every 20 minutes and filtered using a nylon syringe filter of pore size 1.22µm and then analysed by LC-MS. The instrumentation and chromatographic conditions used were as follows; the LC-MS instrument used was a 5600 AB SCIEX Triple TOF hybrid mass spectrometer (Applied Bio systems Sciex, USA) equipped with a high performance Agilent 1260 infinity liquid chromatography

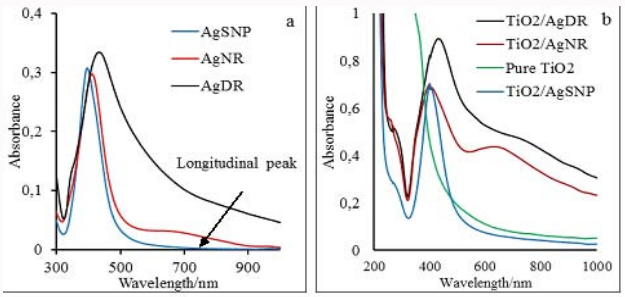

Figure 2: UV-Vis absorption spectra of (a) colloidal AgNR, AgDR and AgSNP and (b) colloidal pure TiO_2, TiO_2/AgNR, TiO_2/AgDR and TiO_2/AgSNP.

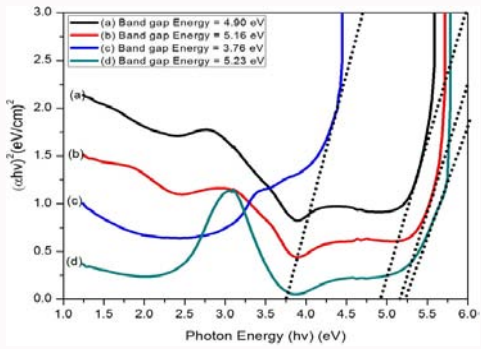

Figure 3: Tauc plots of (a) TiO_2/AgDR; (b) TiO_2/AgNR; (c) pure TiO_2 and (d) TiO_2/AgSNP photocatalysts.

system and operated in the positive turbo ion spray (ESI) mode. The LC chromatography was fitted with a 4.6 x 50 mm reverse phase column Proshell 120; EC-C18 with diameter 7µm. The mobile phase used was composed of two solvents; (Solvent A-water with 0.1% formic acid; Solvent B- acetonitrile with 0.1% formic acid). Bound compounds were eluted at a given gradient. The elution gradient was as follows: the mobile phase started with 5% of acetonitrile, which was increased linearly to 95% in 10 minutes and kept constant for 1 minute and finally returned to the initial conditions in 0.5 minutes and kept constant for 5 minutes giving a total run time of 17 minutes. The column was equilibrated for 5 minutes and the flow rate was $0.5mLmin^{-1}$.

Sample characterisation

The UV-Vis spectra of colloidal solution of silver nanomaterials were obtained using a Perkin Elmer Lambda 35 UV-Vis spectrometer. The structure and morphology of the nanoparticles were determined using high resolution transmission electron microscopy (HRTEM). The analysis was done on a FEI Tecnai F20 field emission gun HRTEM operated at 200kV in bright field mode and the images were collected on a Gatan Ultrascan 2000 CCD camera. The aliquots from the photodegradation solution were analysed by FTIR to establish the changes in the functional groups during the photocatalytic process. The FTIR analysis was done by mixing a drop of the sample with KBr followed by pressing into a pellet which was then analysed.

Results and Discussion

Transmission electron microscopy (TEM) analysis

The prepared silver dendrites had trunks that all grew from the centre spreading outwards forming a star or flower like structure. As the branches grew from the trunks, they overlapped or joined other branches from other trunks forming a relatively dense network as shown in the HRTEM images (Figure 1a). Individual dendrites were observed to be three dimensional and having some branches that were connected to one main trunk in a regular pattern. The angles between the branches and the trunk were not the same; they varied approximately between 45° and 60°. A closer look at the structures showed that some small branches also grew on some of the previously formed branches. The mechanism of growth of these dendrites in this way is not fully understood.

The silver dendrites were the biggest nanostructures with branches that are about 300nm in length and having smaller branches which are 100nm long and 40nm wide (Figure 1a). The TiO_2 nanoparticles (Figure 1b) exhibited different shapes (i.e. square, rectangular, hexagonal and spherical) with particle size ranging from 20nm to 75nm. The spherical silver nanoparticles (Figure 1c) ranged from 5nm to 18nm in size. From the HRTEM image (Figure 1d); it could be observed that the silver nanorods were almost of the same size. Their lengths were between 51.22nm and 82.83nm and their width was approximately 15.86nm.

UV-V is analysis

The UV-Visible absorption spectra of colloidal spherical silver nanoparticles (AgSNP), silver nanorods and silver dendrites show absorption peaks in the range 400nm to 450nm (Figure 2a). The spectrum of the silver nanorods showed two absorption peaks, a sharp one at 405nm and a broad one around 690nm due to transverse oscillation and longitudinal oscillations respectively. This observation is in agreement with available literature [13]. The spherical silver nanoparticles showed a sharp peak centred at 401nm. The peak for the silver dendrites was broad and shifted to higher wavelength (442nm) in comparison to that for spherical silver nanoparticles. This was due to the bigger size of the dendritic nanostructures. Figure 2b shows the UV-Vis absorption spectra of pure TiO_2 and the composite materials. The absorption peak for TiO_2/AgSNP centred at 395nm showed a blue shift in comparison to pure spherical silver nanoparticles (401nm) due to TiO_2 which absorbs strongly in the UV region. This was also observed in other samples where the spectra blue shifted from 442nm in AgDR to 440nm in TiO_2/AgDR and from 405nm in AgNR to 399nm in TiO_2/AgNR. The absorption edge of pure TiO_2 was found at 388nm. Hence the combination of TiO_2 and silver nanostructures blue shifts the absorption spectra of silver and red shifts the absorption edge of TiO_2.

The Tauc plots of the composite photocatalysts are shown in Figure 3. The band gap values followed the order; pure TiO_2 > TiO_2/AgDR > TiO_2/AgNR > TiO_2/AgSNP. From the HRTEM images the particle sizes also follow the same trend hence the reason for the observed trend in band gap values could be due to quantum confinement effects.

XRD analysis

The XRD patterns of TiO_2, TiO_2/AgSNP, TiO_2/AgNR and TiO_2/AgDR are shown in Figure 4. Four silver peaks observed at 38.02°, 44.3°, 64.3° and 77.5° were indexed to the diffraction of (111), (200), (220) and (311) planes assigned to face centred cubic (fcc) structure (JCPDS No: 04-0783). All the peaks due to silver were small since the composites were mainly composed of titanium dioxide and had only 0.5% (w/w) of silver. The peak at 32.1° and 46.1° in the XRD pattern of TiO_2/AgSNP and TiO_2/AgNR were due to chlorargyrite (JCPDDS, File No. 31-1238). Its formation could be due to the reaction of silver with traces of chloride ions in TiO_2 since titanium tetrachloride was

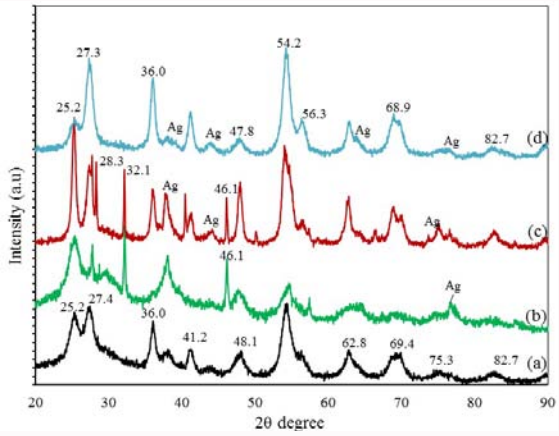

Figure 4: XRD patterns of (a) TiO_2; (b) TiO_2/AgSNP; (c) TiO_2/AgNR and (d) TiO_2/AgDR.

used for the synthesis of TiO_2. The peaks at 2θ 25.2˚, 47.8˚, 56.3˚, 68.9˚, 62.8˚ and 82.7˚ correspond to (101), (200), (211), (116) and (224) crystal faces of anatase phase of TiO_2 [14]. The peaks at 27.3˚, 36.0˚ and 41.3˚ were due to (110), (101) and (200) mirror planes of the rutile phase of TiO_2. Generally, all the composites have both anatase and rutile phases of TiO_2. In TiO_2/AgSNP and TiO_2/AgNR samples, there was more anatase phase than the rutile phase whereas in TiO_2/AgNR there was more rutile phase than the anatase phase.

Photocatalytic activity evaluation

All the TiO_2/Ag composite materials showed higher photocatalytic activities than pure TiO_2 photocatalyst (Figure 5). The highest TiO_2 photocatalyst enhancement was achieved by spherical silver nanoparticles where 80.98% of methyl orange was degraded after 300 minutes followed by silver nanorods with 70.55% and lastly silver dendrites with 64.78%. The observed trend of enhancement can be attributed to the differences in size and shape of the silver nanostructures. According to literature, photocatalytic reactions occur at active sites on the surface of the nanoparticles, hence size is of great essence [15]. The smaller the Ag nanostructures the greater the surface area that would be available for contact with TiO_2 and this promotes electron transfer resulting in low electron-hole recombination rates. Literature states that one-dimensional structures (silver nanorods and silver dendrites) possess similar advantages to zero dimensional nanoparticles (spherical silver nanoparticles) [16,17]. Morphology and size have a huge influence on surface area to volume ratio of the photocatalyst material. The superior performance of AgSNP is supported by TEM average particle sizes (about 11nm) which entail high surface area to volume ratio compared to silver nanorods (15.86nm in width) and silver dentrites (40nm wide). The other reason for the observed trend could be the differences in the wavelengths at which the Ag nanostructures absorb light. The zero dimensional spherical nanoparticles absorb at lower wavelength when compared to one dimensional AgNR with maximum absorption at 405nm (Figure 2) and dendritic nanostructures with maximum absorption at 444nm (Figure 2). Since the experiments were conducted under UV light, AgSNP with the highest band gap (Figure 3) absorbed more light than both AgNR and AgDR resulting in more localized surface plasmon resonance (LSPR) which aided photocatalysis. The XRD crystal structure information also augments the finding that the AgSNP exhibited the highest photocatalytic activity. This is attributed to the high content of the anatase phase of

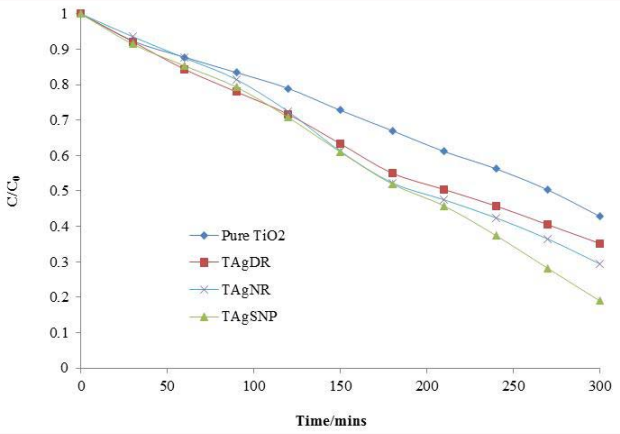

Figure 5: Photodegradation curves of methyl orange using nanocomposites of TiO_2 and Ag nanostructures of different shapes at 25˚C and pH 7 under UV light.

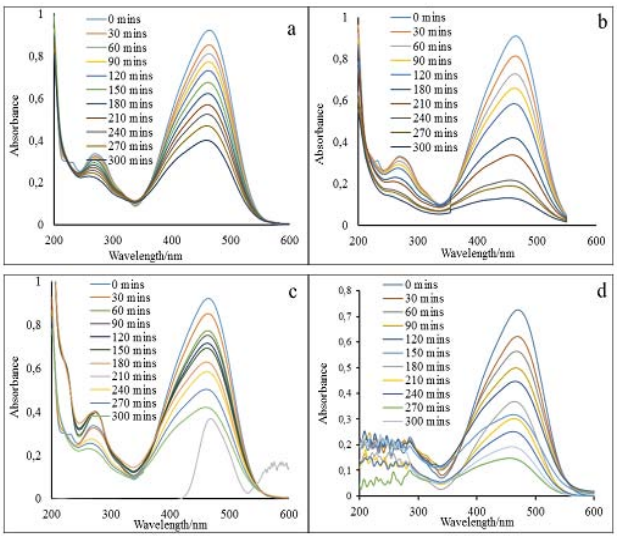

Figure 6: UV/Vis absorption spectra for the photodegradation of methyl orange using (a) pure TiO_2, (b) TAgSNP, (c) TAgDR and (d) TAgNR under UV light illumination.

TiO_2 which is known to present high photoactivity compared to the rutile phase [15].

The spectra of methyl orange solution before and during photocatalytic degradation experiments were are shown in Figure 6. The intensity of the absorption peak at 464nm decreased with increase in photodegration time. There were no observable changes in the line shape of the spectra. It is important to note that the methyl orange was stable under UV illumination as no changes in concentration were observed after illumination in the absence of the photocatalyst.

Determination of photodegradation products

Methyl orange in solution is an anionic compound and in most LC-MS studies it has been analysed in the negative mode. In this study it has been analysed in the positive mode so as to study the possibility of identifying new photodegradation products. When it is analyzed in the positive mode, it is protonated on the SO_3- group to make it neutral and then gains another proton to give a detectable characteristic positive molecular adduct $[M + H]^+$. The molecular mass calculator of the instrument was used to determine the m/z

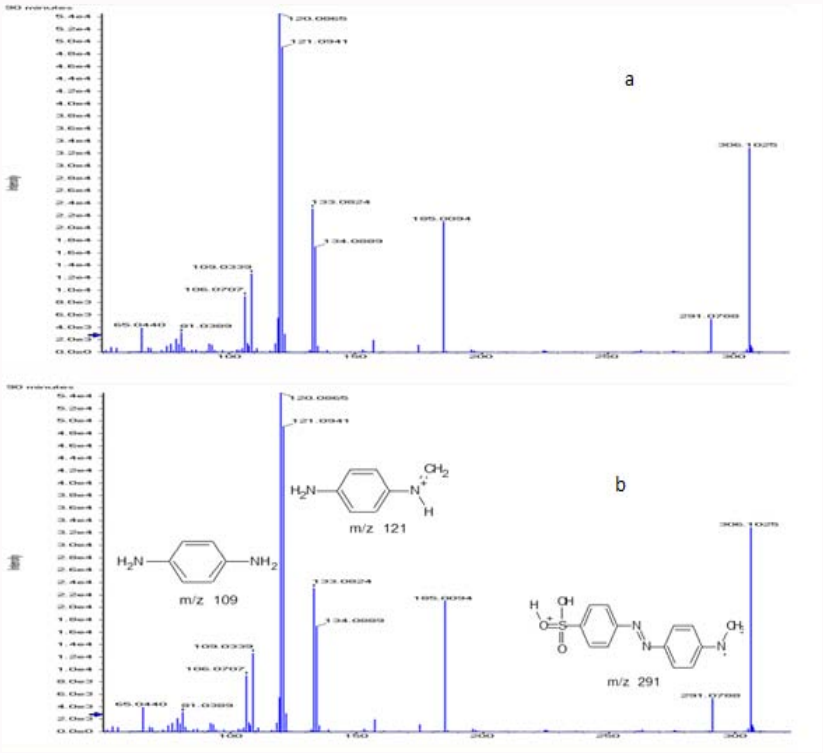

Figure 7: Positive-ion MS-MS of methyl orange at (a) zero minutes and (b) 90 minutes.

of the parent molecule, which was 306. The LC-MS elution spectra obtained for the photo-degradation of methyl orange at different photo-degradation times (0, 30, 60, 90 and 300 minutes) are shown in Figure 7. The MS/MS spectra of the methyl orange at zero minutes and after 90 minutes are shown in Figure 7. The signal at m/z 306 was due to the positive ion of the parent molecule. The MS/MS analysis of this ion gave at least ten significant m/z values of 65.04, 81.03, 101.03, 120.08, 121.09, 133.08, 134.08, 185.01 and 291.07. A visualization of the results of the possible intermediates formed based on the bonds that were more susceptible to breakdown is shown in Figure 4. In this study it was observed that homolytic bond breaking became competitive irrespective of the absence of stabilization of an odd electron. This was shown in the formation of the fragment with m/z of 291. The possible intermediates suggested in this study were not the only ones present in the photodegradation solution as some possible structures could not be deduced from the given m/z values. To the best of our knowledge, this was the first LC-MS analysis of the photodegradation products of methyl orange in the positive mode. Most researchers analysed it in the negative mode as it easily loses the sodium ion in solution and becomes negatively charged. When compared with previous studies [18,19] carried out in the negative mode, this study detected different intermediates (Figure 8).

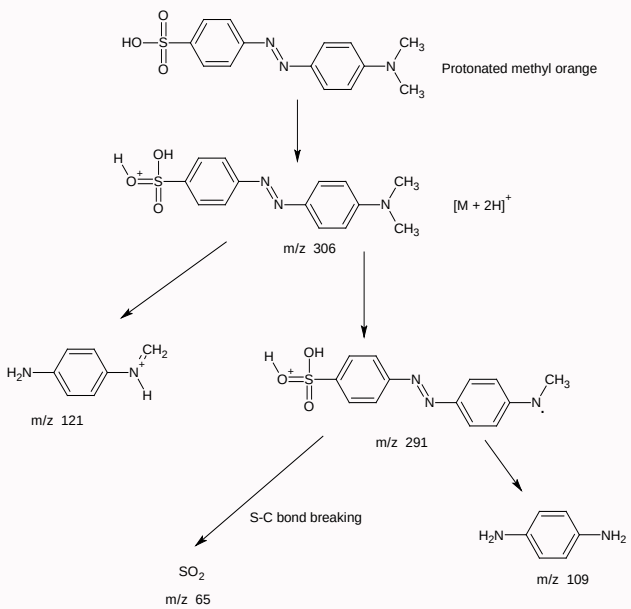

Figure 8: Proposed photodegradation pathway and some of the intermediates of methyl orange.

FTIR analysis of degradation products

The photodegradation of methyl orange was also studied using FTIR whereby the analysis was done on a 10ppm methyl orange solution before degradation and after every hour for 30 minutes of photodegradation. This analysis gave an idea on the way the methyl orange was photodegraded in terms of which bonds were cleaved. This was observed in the decrease in the intensity of certain characteristic peaks of some functional groups (Figure 9). The characteristic peaks due to the C-H stretching of the methyl groups around wavenumber 2978cm^{-1} and 2899cm^{-1} found in the spectrum of the initial methyl orange were seen to have almost disappeared in the spectrum of the photodegraded methyl orange extract after 5 hours. This could be due to the fragmentation and destruction of the methyl groups from the parent methyl orange molecule. In the spectra of the extracts, the peaks at 1395cm^{-1} (C-H stretching of methyl), 1246cm^{-1} (=C-N stretching) and 1052cm^{-1} (C-N stretch) significantly decreased compared to the spectrum of the initial methyl orange. This showed that the functional groups that gave rise to those peaks had been degraded to some extent with the major degradation or cleavage taking place on the C-N

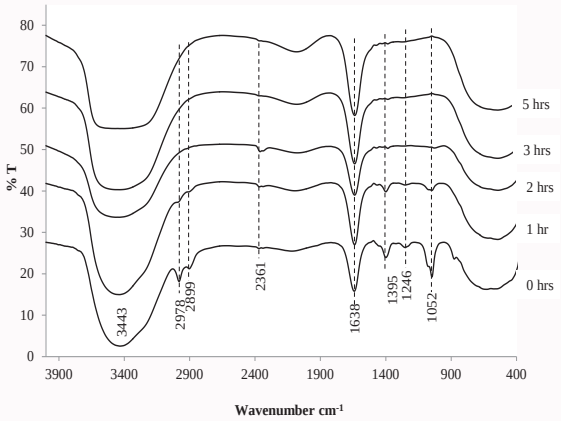

Figure 9: FTIR spectra of methyl orange at different stages of photo-degradation.

bonds as evidenced by the major decrease in the C-N peak at 1052cm^{-1}. The peak at 876cm^{-1} (=C-H bending) completely disappeared after photodegradation implying the complete destruction of the groups giving rise to that peak. The breakdown of the C-N bond was faster than that for C-C bonds as evidenced by the rate of decrease of the intensity of the corresponding FTIR peaks. Hence it can be concluded that the degradation of methyl orange occurred via an electrophilic attack by the OH$^{\bullet}$ radicals leading to an abstraction of a hydrogen atom and resulting in the cleavage of the C-N bond. A similar mechanism was suggested by other researchers [20] for the degradation of alkanolamines.

Conclusions

This work demonstrated the successful fabrication of Ag/TiO_2 composites with interesting photocatalytic applications. The performance of nanocrystalline TiO_2 photocatalyst can be improved by noble silver nanoparticles by 23.82% under UV light irradiation. The spherical silver nanoparticles enhanced the photocatalytic activity of TiO^2 towards methyl orange more than the nanorods and dendritic silver nanostructures. The study showed that the structure and size of the silver nanomaterials play an important role in determining the extent to which organic contaminants are degraded when used as composites with TiO_2 although it is difficult to produce nanoparticles of the same size. New methyl orange photodegradation intermediates can be detected by LC-MS analysis when the mode of the instrument is changed.

Acknowledgments

The research described in this paper was financially supported by the National Research Foundation of South Africa.

References

1. Cozzoli PD, Fanizza E, Comparelli R, Curri ML and Agostiano A. Role of Metal Nanoparticles in TiO_2/Ag nanocomposite-based microheterogeneous photocatalysis. J Phys Chem B. 2004; 108: 9623-9630.
2. Nagaveni K, Sivalingam G, Hegde MS and Madras G. Photocatalytic degradation of organic compounds over combustion-synthesized nano-TiO_2. Environ. Sci. Tech. 2004; 38: 1600-1604.
3. Borges ME, Sierra M, Méndez-Ramos J, Acosta-Mora P, Ruiz-Morales JC and Esparza P. Solar degradation of contaminants in water: TiO_2 solar photocatalysis assisted by up-conversion luminescent materials. Sol. Ener. Mater. Sol. Cells. 2016; 155: 194-201.
4. Kumar M, Parasha KK, Tandi SK, Kumar T, Agarwal DC and Pathak A. Fabrication of Ag: TiO_2 nanocomposite thin films by sol-gel followed by electron beam physical vapour deposition technique. 2013; 2013: 1-6.
5. Malagutti AR, Mourão HAJL, Garbin JR and Ribeiro C. Deposition of TiO_2 and Ag: TiO_2 thin films by the polymeric precursor method and their application in the photodegradation of textile dyes. Appl. Catal. B. 2009; 90: 205-212.
6. Li N, Zhang X, Yuan S, Zhang X, Yuan Y and Li X. (Hollow Au-Ag nanoparticles)-TiO_2 composites for improved photocatalytic activity prepared from block copolymer-stabilized bimetallic nanoparticles. Phys. Chem. Chem. Phys. 2015; 17: 12023-12030.
7. Zhang D. Improved visible light photocatalytic activity of titania loaded with silver on discoloration of a heterocyclic aromatic chemical dye solution. Russian J. Phys. Chem A. 2012; 86: 675-680.
8. Nyamukamba P, Tichagwa L, Ngila JC and Petrik L. Plasmon decorated titanium dioxide thin films for enhanced photodegradation of organic contaminants. J. Photochem. Photobio. A: Chem. 2017; 343: 85-95.
9. Rosu MC, Socaci C, Avram VF, Borodi G, Pogacean F, Coros M, et al. Photocatalytic performance of graphene/TiO_2-Ag composites on amaranth dye degradation. Mater. Chem. Phys. 2016; 179: 232-241.
10. Gao L, Gan W, Xiao S, Zhan X and Li J. A robust superhydrophobic antibacterial Ag-TiO_2 composite film immobilized on wood substrate for photodegradation of phenol under visible-light illumination. Ceram. Int. 2016; 42: 2170-2179.
11. Mungondori HH and Tichagwa L. Photo-catalytic activity of carbon/nitrogen doped TiO_2-SiO_2 under UV and visible light irradiation. Mater. Sci. Forum. 2013; 734: 226-236.
12. Markelonis AR, Wang JS, Ullrich B, Wai CM and Brown GJ. Nanoparticle film deposition using a simple and fast centrifuge sedimentation method. Appl. Nano. 2015; 5: 457-468.
13. Ojha AK, Forster S, Kumar S, Vats S, Negi S and Fischer I. Synthesis of well–dispersed silver nanorods of different aspect ratios and their antimicrobial properties against gram positive and negative bacterial strains. J. Nanobiotech. 2013; 11: 42.
14. An G, Yang C, Zhou Y and Zhao X. Plasmon-enhanced photoluminescence from TiO_2:Sm3R: Au nanostructure. Phys. Stat. Sol. A. 2012; 209: 2583-2588.
15. Verbruggen SW. TiO_2 photocatalysis for the degradation of pollutants in gas phase: From morphological design to plasmonic enhancement. J. Photochem. Photobiol. C: Photochem. Rev. 2015; 24: 64-82.
16. Yuan Y, Zhao Y, Li H, Li Y, Gao X, Zheng C, et al. Electrospun metal oxide-TiO_2 nanofibers for elemental mercury removal from flue gas. J. Hazard. Mater. 2012; 227-228: 427-435.
17. Wu Z, Dong F, Zhao W, Wang H, Liu Y and Guan B. The fabrication and characterization of novel carbon doped TiO_2 nanotubes, nanowires and nanorods with high visible light photocatalytic activity. Nanotech. 2009; 20: 235701.
18. Baiocchi C, Brussino MC, Pramauro E, Prevot AB, Palmisano L and Marc G. Characterization of methyl orange and its photocatalytic degradation products by HPLC/UV-VIS diode array and atmospheric pressure ionization quadrupole ion trap mass spectrometry. Int. J. Mass Spec. 2002, 214: 247-256.
19. Hisaindee S, Meetani MA and Rauf MA. Application of LC-MS to the analysis of advanced oxidation process (AOP) degradation of dye products and reaction mechanisms. Trends in Anal. Chem. 2013; 49: 31-44.
20. Klare M, Scheen J, Vogelsang K, Jacobs H and Broekaert JAC. Degradation of short-chain alkyl- and alkanolamines by TiO_2- and Pt/TiO_2-assisted photo-catalysis. Chemos. 2000; 41: 353-362.